ICREN-01/2013 February 16-16, 2013 Constantine, Algeria
First International Conference o7n Renewable Energies and Nanotechnology impact on Medicine and Ecology

# The effect of porous media thickness and the air velocity inlet on the temperature distribution inside a solar tower volumetric receiver

Mohamed Mammar[a], Abderrahmane Hamidat[a]

[a]*Development Center of Renewable Energy (CDER), BP. 62 Route de l'Observatoire Bouzaréah, Algiers, Algeria*

**Abstract**

In order to investigate the steady heat transfer characteristics of a porous media solar tower receiver, this paper applies the steady heat and mass transfer models of the porous media to solar receivers, chooses the preferable volume convection heat transfer coefficient model, solves these equations by using the numerical method of finite volume, and analyzes the typical influences of the thickness and the air velocity inlet, on the temperature distribution. The paper can provide a reference for this type of receiver design and reconstruction.
Finite volume method was used to solve the governing equations. Upwind scheme was applied to governing equations, and solution was obtained using the Gausse-Seidel iterative method. The computational domain was discretized by (50 x1) grids. The convergence criterion was to be 10-3 relative error between consecutive iterations for the grid points in the calculation domain. The inlet air temperature was set to 293 K and a uniform solar radiation flux, qw, was set to 1 MW/m2. Constant properties of the fluid and porous media were assumed for air and SiC matrix.

*Keywords*: Numeric investigation, finite volume method, porous media, solar tower

## 1. Introduction

The increasing problems of CO2 emissions and energy security concerns have strengthened interest in alternative, nonpetroleum-based sources of energy. STPP with optical concentration technologies are important candidates for becoming a major clean renewable energy resource in the medium-term [1]. The development of these power plants has been associated to the adaptation of proven steam power generation technologies combined with particular concentrating solar power components [2].
STPP are a recognized option for large scale renewable electricity production. In these systems, direct solar radiation is concentrated onto an absorbing surface, where it is transformed into heat at high temperature levels, which in turn is used in a thermodynamic cycle driving a generator to produce electricity. Dispatchable power can be provided to the utility grid by means of integrated thermal storage and/or fuel based back-up systems [3].

* Mohamed Mammar, Abderrahmane Hamidat. Tel: +213 21 90 15 03/ 90 14 46
; fax: +213 21 90 15 60/ 90 16 54.
*E-mail address*: Mohamed.mammar@cder.dz/mammar82yahoo.fr

**Nomenclature**

| | |
|---|---|
| A | radius of |
| B | position of |
| C | further nomenclature continues down the page inside the text box |
| CDER | the center for Renewable energy development |
| STPP | solar thermal power plant |
| SPT | solar power tower |
| CRS | central receiver system |
| $\rho_f$ | fluid density |
| $u$ | velocity in streamwise (x-direction) |
| $v$ | velocity cross-stream (y-direction) |
| $T_f$ | solid matrix temperatures |
| $T_s$ | solid matrix temperatures |
| $c_f$ | specific heat |
| $\lambda_f$ | Thermal conductivity |
| $\lambda_{f,eff}$ | Effective thermal conductivity of the fluid |
| $\lambda_s$ | Thermal conductivity of the solid matrix |
| $\lambda_{s,eff}$ | Effective thermal conductivity of the fluid |
| $\varepsilon$ | Porosity |
| $h_v$ | Volumetric convection heat transfer coefficient |
| $\mathrm{d_p}$ | Average particle diameter of the porous media |
| $h_{sf}$ | heat transfer coefficient |
| $a_{sf}$ | specific surface area of per unit volume |
| $u_0$ | velocity inlet |
| $\mu_f$ | dynamic viscosity |

| | |
|---|---|
| $Re_d$ | Reynolds number |
| $T_{f0}$ | fluid inlet temperature |
| $q_w$ | heat flux absorbed by the receive |

Four general approaches have received development attention [4]: Parabolic trough, Fresnel collector, solar dish and solar tower – all are solar thermal concentrated power plants [5].
The history of using solar energy in Algeria backs to 1954 with the solar furnace built by the French for ceramic fabrication purpose. The insolation time over the quasi-totality of the national territory exceeds 2000 h annually and may reach 3900 h (high plains and Sahara). The daily obtained energy on a horizontal surface of 1m2 is of 5 kWh over the major part of the national territory, or about 1700kWh/m2/year for the North and 2263kWh/m2/year for the South of the country [6]. It is physically suitable for STTP development including the whole of the MENA region.
Algeria fosters research to make of the renewable energy program a catalyst for developing a national industry which will optimize the various Algerian potentials (human, physical, scientific, etc.).
In addition to the research centers affiliated to companies like Electricity and Gas Research and Development Center (CREDEG), which are a subsidiary of Sonelgaz, the energy and mining sector has an Agency for the Promotion and Rational Use of Energy (APRUE) and a company specialized in the development of renewable energy. These bodies which cooperate with the research centers attached to the Ministry of Scientific Research include CDER and UDTS [7].
CDER or Center for Renewable Energy Development is responsible for developing and implementing programs of scientific and technological research and development of systems using solar (Including STPP), wind, geothermal and biomass energies.
The development of solar energy plants is supported by the Ministry of Energy and Mines (MEM) and realised mainly by Sonelgaz and other private installers companies. The solar energy is regarded as an important line of research within the structure of the department of renewable energies. Thus, CDER have a particular collaboration with solar Institute of Jülich (Germany) in order to develop all the categories of solar energy including solar power tower technology.

## 2. Solar thermal energy program in Algeria:

Algeria has created a green momentum by launching an ambitious program to develop renewable energies and promote energy efficiency. In this program, renewable energies are at the heart of Algeria's energy and economic policies: It is expected that about 40% of electricity produced for domestic consumption will be from renewable energy sources by 2030.

The national potential for renewable energy is strongly dominated by solar energy. Algeria considers this source of energy as an opportunity and a lever for economic and social development, particularly through the establishment of wealth and job-creating industries.
The program provides for the development by 2020 of about sixty solar photovoltaic and concentrating solar power plants, wind farms as well as hybrid power plants.
Pilot projects for the construction of two solar power plants with storage of a total capacity of about 150 MW each, will be launched during the 2011-2013 period. These will be in addition to the hybrid power plant project of Hassi R'Mel with a total power capacity of 150 MW, including 25 MW in solar.

Four (4) solar thermal power plants with a total capacity of about 1 200 MW are to be constructed over the period 2016-2020. The 2021-2030 program provides for the installation of an annual capacity of 500 MW until 2023, then 600 MW per year until 2030 [6,7].
The 2011-2013 period will see the launching of studies for the local manufacturing of equipment for the solar thermal sector. The industrial integration rate is expected to reach 50% over the 2014-2020 period through the implementation of three major projects in parallel with actions for engineering capacity building:

- Construction of a mirror manufacturing plant;
- Construction of heat transfer fluid and energy storage equipment factories;
- Construction of a factory for the manufacture of power block equipment;
- Development of engineering activities and design, procurement and production capabilities to achieve an industrial integration capacity rate of at least 50%.

Over the 2021-2030 period, the rate of integration should exceed 80% through the implementation.

## 3. Solar air receiver technology

### *3. 1. Solar power tower plant with solar air receiver*

SPT plant consists of concentrator and receiver unit, heat transfer, exchange and storage unit, transmission and distribution unit, auxiliary unit, integrated control system and so on. Each unit has its independent control modules, and integrated control system assembles every unit as a whole to analyze, coordinate and optimize the function of the system, making sure that the plant can be operated according to the designed control schemes and operating modes under various conditions and running phases and works in a safe, high-efficient, economic and stable way [8].

Particularly high concentrations and therefore high working temperatures as well as efficiencies of the subsequent thermodynamic working processes can be attained in point focusing systems. Fig. 1 shows one of those CRS-Systems, the solar tower power plant [9].
A typical solar tower power system consists of a field of two-axis tracking reflectors, called heliostats, which focus the direct solar radiation onto a tower-mounted receiver [4].
The heliostat field concentrates sunlight to fluxes of 500–1000 suns. This concentration is sufficient to achieve temperatures above 1200 °C on the receiver.
The receiver is located at the top of the tower and acts as an energy exchanger (Fig 1). Receivers are made of material, which can withstand high temperature changes and high energy density [9].

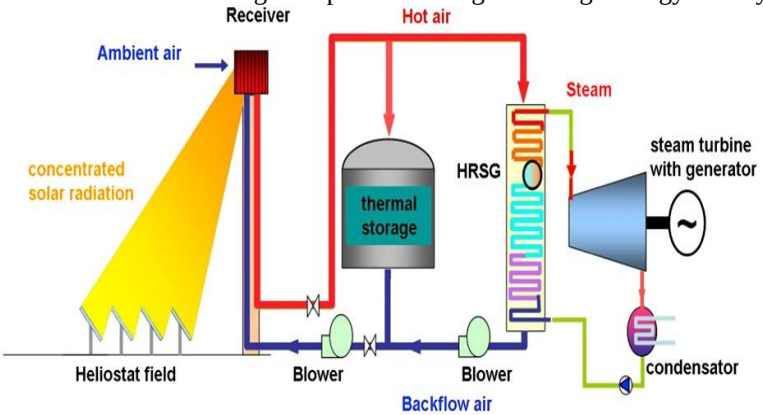


Fig. 1. Schematic diagram of the test and demonstration power plant Julich [5].

Ceramic or metal structures are most suitable for this application. They receive concentrated solar energy and transfer it to heat.
The heat is transported via ambient air to a thermo hydraulic circuit. After heating up in the receiver it is fed into a state-of-the-art heat recovery steam generator.
In this conventional cycle, steam is produced in the boiler and transported to a steam turbine. The steam expands in the turbine producing mechanical work which is then converted into electrical energy through a generator. Exhaust steam from the turbine is condensed in a condenser, and the condensate thereafter pumped to the boiler where it again receives heat from the solar receiver, and the cycle is repeated this thermodynamic cycle driving a generator to produce electricity [9, 3].

### *3.2. Solar air receiver module*

The solar air receiver is often also called volumetric air receiver, because due to the porosity of the material the concentrated solar radiation is absorbed in part of the volume of the material [10]. The receiver consists of many receiver modules (elements), and there are many types of them (Fig. 2.3).

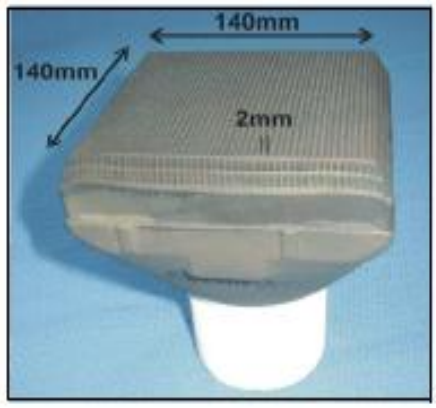


Fig 2. HITREC receiver module [8]

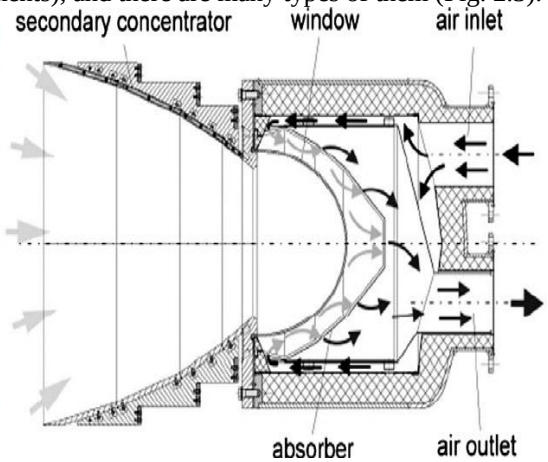


Fig. 3. REFOS receiver module [1].

### *3.3. Operating principles*

Its principle is illustrated in Fig. 4. A simple tubular absorber is shown for comparison. Because cold ambient air enters the material at the front of the volumetric absorber, where it is facing the radiation, the material can be kept relatively cool. In an ideal operation, the temperature distribution should be as shown on the lower right-hand side of Fig. 4. The low temperature level at the front minimizes thermal radiation losses [10].

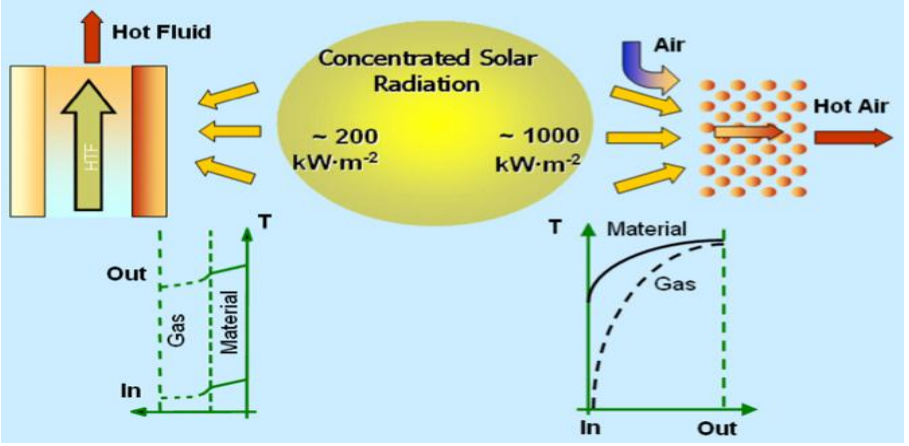


Fig. 4. The volumetric receiver principle compared to a tube receiver [2].

### *3.4. The advantages of volumetric receiver technology*

Most of the solar receivers can be classified as either Indirectly-Irradiated or Directly-Irradiated (Volumetric receiver) [11].
Research and development focused on new receivers for future plants with a smaller aperture to minimize heat loss, allowing higher solar flux compared than technologies in use at the time (tube receiver) [1]. Alternative receivers based on other concepts, such as the volumetric receiver that were simpler, cheaper, and more efficient and had better thermal properties.
Volumetric receivers are more flexible than tube receivers due to their functionality and three-dimensional configuration (volumetric) compared to the quasi-two-dimensional tube.

### *3.5. Types of volumetric absorbers*

The classification based on the combination of two important factors, pressurization and material, resulting in four subgroups with a representative receiver defining each type [1]:

- Phoebus-TSA type: open-loop volumetric receiver with metallic absorber ( Mk-I, Sulzer 1, Sulzer 2, Catrec 1, TSA, Bechtel 1, Bechtel 2, Catrec 2, SIREC).
- SOLAIR type: open-loop volumetric receiver with ceramic absorber (Sandia foam, CeramTec, Conphoebus-Naples, Selective receiver, HiTRec I, HiTRec II, SOLAIR 200, SOLAIR 3000).
- REFOS type: closed-loop volumetric receiver with metallic absorber (REFOS, SOLGATE).
- DIAPR type: closed-loop volumetric receiver with ceramic absorber (PLVCR-5, PLVCR-500, DIAPR 30–50, DIAPR multistage).

#### *3.5.1. Investigated absorber structures*

Volumetric absorber structures can be distinguished by material and geometry. Three major geometrical configurations exist: wire or fiber meshes, (ceramic) foams and regular honeycomb structures [12].

The highly porous structure of volumetric receivers may be metal or ceramic. Since ceramics are the most appropriate materials for achieving the highest air temperatures, this is the most suitable option when temperatures above 800 °C are necessary [1].

*3.5.2. Material technology of ceramic foams*

The ceramic foam samples were produced by the polymer foam replication method at the Institute of Metal Research (IMR) of the Chinese Academy of Sciences (CAS). Five types of as-manufactured specimens (abbreviation: as-foams) were prepared [13]. Three kinds had a mean cell size ranging from 1.35 to 1.55 mm and a porosity ranging from 0.55 to 0.85; two kinds had the same porosity of 0.7, but different cell sizes of 3.36 mm and 4.49 mm (Fig. 5).

Fig. 5. Ceramic foam types

The ranges of the samples used in this study are not sufficient to generalize to all possible parameters, so the used model is based on numerical simulations and not experimental results. This paper reports a numerical analysis that characterizes the performance of SiC foam ceramic receivers.

SiC has high thermal conductivity, strong strength, high thermal shock resistance, and high antioxygenic properties, and it can be molded to form three-dimensional honeycomb-structured receivers [14]. The honeycomb structure was shown to achieve high (volumetric) efficiency convective heat transfer for the solar power tower plant.

## 4. Modeling and simulation

*4.1 Problem description*

The foam ceramic receiver surface absorbs the solar thermal radiation. The heat is conducted along the solid matrix. When air passes through the porous media, heat is transferred from solid matrix to air. The flow and heat transfer can be simplified to one dimension. The heat transfer process is described in Fig. 6.

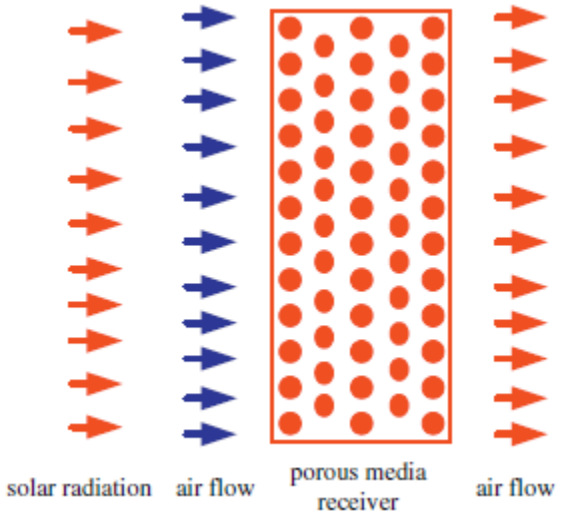


Fig. 6. Flow and heat transfer schematic in a solar porous media receiver [14].

The main assumptions behind the mathematical model are:

- One dimension flow and heat transfer,
- Steady and incompressible flow,
- Homogeneous properties of the gas and solid phase,
- Constant properties of the gas and solid phase.

The thermal equilibrium assumption is not made. Conversely, the gas and solid phases can be at different temperatures, and the local thermal non-quilibrium equations are used. The resultant transport models are as follows.

*4.2 Mathematical model*

*4.2.1 Continuity equation*

$$\frac{\partial(u\rho_f)}{\partial x} + \frac{\partial(v\rho_f)}{\partial y} = 0 \tag{1}$$

Where $\rho_f$ is the fluid density; $u$ and $v$ are velocities in streamwise (x-direction) and cross-stream direction (y-direction).
Using the above assumptions, the continuity equation becomes:

$$\frac{\partial(u\rho_f)}{\partial x} = 0 \quad \text{Or} \quad u = Constant \tag{2}$$

*4.2.2 Momentum equation*

The momentum exchange in porous media was calculated by Brinkmane-Forchheimer Extended Darcy equation. Velocity field is known from the continuity equation, we need only to resolve energy equation with knowing velocity field in order to determinate the temperature distribution.

*4.2.3 Energy equation*

The energy equations for the fluid and solid phase are given respectively in Eqs. (3) and (4). The simplest possible case is treated [14]. Here, a steady one-dimensional case in which the convection, diffusion and source terms are presented. The governing differential equations are:

$$\frac{\partial(c_f \rho_f u T_f)}{\partial x} = \lambda_{f,eff}\left(\frac{\partial^2 T_f}{\partial x^2}\right) + h_v(T_s - T_f) \quad (3)$$

$$\lambda_{s,eff}\left(\frac{\partial^2 T_s}{\partial x^2}\right) - h_v(T_s - T_f) = 0 \quad (4)$$

Whereas;

$$\lambda_{f,eff} = \varepsilon\lambda_f, \lambda_{s,eff} = (1-\varepsilon)\lambda_s \quad (5)$$

The properties for air are denoted by subscript f, and for SiC matrix are denoted by subscript s.

In above equations, $T_f$ and $T_s$ are, respectively, the fluid and solid matrix temperatures; $c_f$ is the specific heat , $\lambda_f$ and $\lambda_{f,eff}$ are the thermal conductivity and the effective thermal conductivity of the fluid, $\lambda_s$ and $\lambda_{s,eff}$ are the thermal conductivity and the effective thermal conductivity of the solid matrix, $\varepsilon$ is the porosity, $h_v$ is the volumetric convection heat transfer coefficient between the fluid and the porous matrix in [W/m3K].

*4.2.4. Application of B. Achenbach Model*

The volumetric convection heat transfer coefficient $h_v$ is calculated using B. Achenbach Model as follows [14]:

$$h_v = h_{sf}\alpha_{sf} \quad (6)$$

Where;

$$h_{sf} = \left[\left(1.18\ Re_d^{0.58}\right)^4 + \left(0.23\ Re_h^{0.75}\right)^4\right]^{\frac{1}{4}} / (d_p \lambda_f) \quad (7)$$

And;

$$\alpha_{sf} = 6(1-\varepsilon)/d_p \quad (8)$$

Whereas;

$$Re_h = Re_d/(1-\varepsilon) \quad (9)$$

$$u_p = u_0/\varepsilon \quad (10)$$

$$Re_d = \varepsilon\rho_f u_p/\mu_f \quad (11)$$

Where $h_{sf}$ is the heat transfer coefficient between the fluid and the porous matrix in [W/m2K] and $\alpha_{sf}$ is the specific surface area of per unit volume in [1/m], $u_0$ is velocity inlet, $\mu_f$ is the dynamic viscosity of the fluid and $Re_d$ is Reynolds number.

*4.2.5. Boundary condition*

Prescribed fluid temperature and wall heat flux are given at the inlet (x=0), Eq. (12), and zero temperature gradient at the exit (x=L), Eq. (13):
If x=0:

$$T_f = T_{f0} \tag{12.a}$$

$$q_w = -\lambda_{s,eff}\left(\frac{\partial T_s}{\partial x}\right) - \lambda_{f,eff}\left(\frac{\partial T_f}{\partial x}\right) \approx -\lambda_{s,eff}\left(\frac{\partial T_s}{\partial x}\right) \tag{12.b}$$

Where: $\left(\lambda_{s,eff} \ll \lambda_{f,eff}\right)$

If x=L:

$$\frac{\partial T_f}{\partial x} = \frac{\partial T_s}{\partial x} = 0 \tag{13}$$

In Eq. (12.a), $T_{f0}$ is the prescribed (constant) fluid inlet temperature and $q_w$ is the heat flux absorbed by the receiver.

*4.3 Numerical method*

The convection is created by the fluid flow. Our task is to obtain a solution for Tf in the presence of given flow field u=constant. However, Finite volume method was used to solve the governing equations. Upwind scheme was applied, and solution was obtained using the Gausse-Seidel iterative method. The computational domain was discretized by (50 x1) grids. The convergence criterion was to be 10-3 relative error between consecutive iterations for the grid points in the calculation domain. The inlet air temperature was set to 293 K and a uniform solar radiation flux, $q_w$, was set at the entrance. Constant properties of the fluid and porous media were assumed for air and SiC matrix.

$\rho_f = 1.225\ \text{kg/m}^3$, $c_f = 1006\ \text{J/(kg.K)}$; $\lambda_f = 0.0242\ \text{W/(m.K)}$;
$\mu_f = 1.8199 \times 10^{-5}\ \text{Pa s}$.

*4.3.1 Discretization of equations*

The discretization of the energy and continuity equations was accomplished using a fully conservative finite-volume method on a structured grid $\Delta x = (\delta x)_w = (\delta x)_e$.

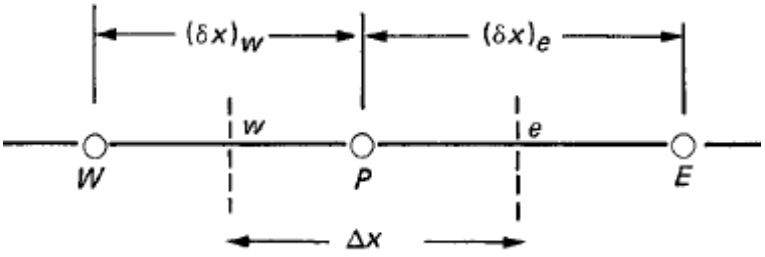


Figure 7: Grid-point cluster for the one-dimensional problem.

For deriving the discretization equation, we shall use the three-grid-point cluster shown in Fig. 7. Although the actual location of the control-volume faces $e$ and $w$ would not influence our final

formulation [15], it is convenient to assume that $e$ is located midway between $P$ and $E$, and $w$ midway between $W$ and $P$.

*4.3.2 Discretization of energy equation for the fluid (The Upwind Scheme)*

The upwind scheme recognizes that the weak point in the preliminary formulation is the assumption that the convected property $T_{fe}$ at the interface is the average of $T_{fE}$ and $T_{fP}$, and it proposes a better prescription. The formulation of the diffusion term is left unchanged, but the convection term is calculated from the following assumption:

The value of $T_f$ at an interface is equal to the value of $T_f$ at the grid point on the upwind side of the face [15].

We define four symbols $F$, $D$, $S_C$ and $S_P$ as follows:

$$F = c_f \rho_f u, \; D = \frac{\lambda_{f,eff}}{\Delta x}, \tag{14}$$

The quantities $S_C$ and $S_P$ arise from the source-term linearization of the form:

$$S = S_C + S_p T_p = h_v \left(T_{fP} - T_{sP}\right) \tag{15}$$

Where;

$$S_C = h_v \, T_s, \; S_p = -h_v \tag{16}$$

$T_{fe}$ is defined as following,

$$T_{fe} = T_{fP} \text{ if } F_e > 0 \tag{17.a}$$

$$T_{fe} = T_{fE} \text{ if } F_e < 0 \tag{17.b}$$

The value of $T_{fw}$ can be defined similarly.

The conditional statements (17.a) and (17.b) can be more compactly written if we define a new operator. We shall define $[\![A, B]\!]$ to denote the greater of A and B. Then , the upwind sheme implies

$$F_e T_{fe} = T_{fP} [\![F_e, 0]\!] - T_{fE} [\![-F_e, 0]\!] \tag{17.c}$$

When the equation (3) is replaced by this concept, the discretization equation becomes:

$$a_P T_{fP} = a_E T_{fE} + a_W T_{fW} + b \tag{18}$$

Where;

$$a_E = D_e + [\![-F_e, 0]\!] \tag{19}$$

$$a_W = D_W + [\![F_w, 0]\!] \tag{20}$$

And;

$$b = S_C \, \Delta x \tag{21}$$

Where;

$$a_p = D_e + [\![F_e, 0]\!] + D_w + [\![-F_w, 0]\!] - S_p \, \Delta x$$
$$= a_E + a_W + (F_e - F_w) - S_p \, \Delta x \tag{22}$$

*4.3.3 Discretization of Solid energy equation*

The discretisation of the equation (4) is [13]:

$$a_p T_{fp} = a_E T_{sE} + a_W T_{sW} + b \tag{23}$$

Where;

$$a_E = \frac{\lambda_{s,eff}}{\Delta x} \tag{24}$$

$$a_W = \frac{\lambda_{s,eff}}{\Delta x} \tag{25}$$

$$a_p = a_E + a_W - S_p \ \Delta x \tag{26}$$

And;

$$b = S_C \, \Delta x \tag{27}$$

*4.3.4 The boundary discretization*

The boundary temperature is not given for the solid matrix; we need to construct an additional equation for $T_{sB}$. This is done by interrgrating the differential equation over the half control volume extends only on one side of the grid point B. This is why we refer to it as the half control volume. An enlarged view of this control volume is given in Fig 8. Integrating Eq (4) over this control volume and noting that flux $q_w$ stands for $-\lambda_{s,eff}\left(\frac{\partial T_s}{\partial x}\right)$ (see eq. 12.b), we get

$$q_B - q_i + (S_C + S_p T_{sB}) \, \Delta x = 0 \tag{29}$$

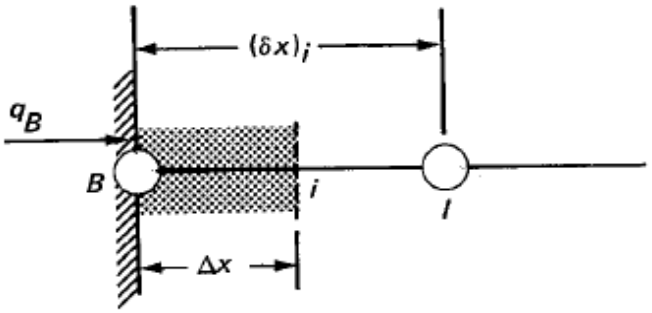


Figure 8: half control volume near the boundary.

Where; the source term has been linearized in usual fashion. The interface heat flux $q_i$ can be written along the lines of eq. (30).

$$q_i = \frac{\lambda_{s,eff}(T_{sB} - T_{sI})}{(\delta x)_i} \tag{30}$$

The results is

$$q_B - \frac{\lambda_{s,eff}(T_{sB} - T_{sI})}{(\delta x)_i} + (S_C + S_p\, T_{sB})\, \Delta x = 0 \tag{31}$$

Where:

$$(\delta x)_i = 2\, \Delta x \tag{32}$$

The required equation for $T_{sB}$ becomes:

$$a_B T_{sB} = a_I T_{sI} + b \tag{33}$$

Where;

$$a_I = \frac{\lambda_{s,eff}}{(\delta x)_i} \tag{34}$$

$$b = S_C\, \Delta x + q_B \tag{35}$$

$$a_B = a_I - S_p \Delta x \tag{36}$$

In this manner we are able to construct the required number of equations for the unknown temperatures.

The boundary discritization at the outlet $(x = L: \frac{\partial T_f}{\partial x} = \frac{\partial T_s}{\partial x} = 0)$ can be defined similarly with $q_w = 0$.

## 5. Results and discussion

Results calculated based on B. Achenbach model summarized above in the equations (6-11), we analyze the typical influences of the inlet heat flux, thermal conductivity, porosity, receiver thickness, and air inlet velocity on the temperature distributions.

### *5.4. Effects of receiver thickness*

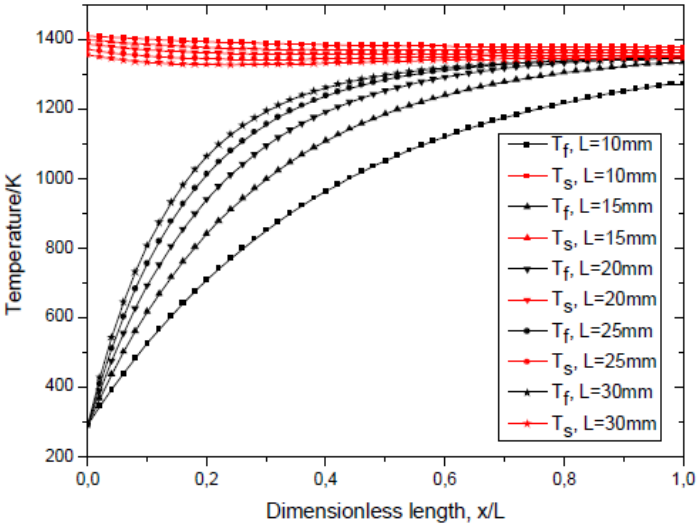


*Fig.* 12. The influence of thickness on the temperature distribution; $\varepsilon = 0.25, u_0 = 1m/s, d_p = 0.025mm$, $qw = 1MW/m^2, \lambda_s = 118W/(m-K)$.

The effects of air receiver thickness on the temperature profiles are shown in Fig. 12. Five receiver thicknesses, 10, 15, 20, 25 and 30 mm, were examined. The remaining parameters were kept unchanged from those used in Fig. 9. The temperature of the solid matrix decreases slightly along the air flow direction; and the air temperature increases rapidly along the flow direction.
The solid temperatures decrease and the air temperature increase with increasing the thickness, in which the temperature difference between the solid and the fluid decreases with increasing thickness.
The temperature of the solid matrix at the absorbing surface is 1410,8 K when the thickness is set to 10 mm, whereas it is 1356,4 when the thickness is 30 mm.

*5.5. Effects of air inlet velocity*

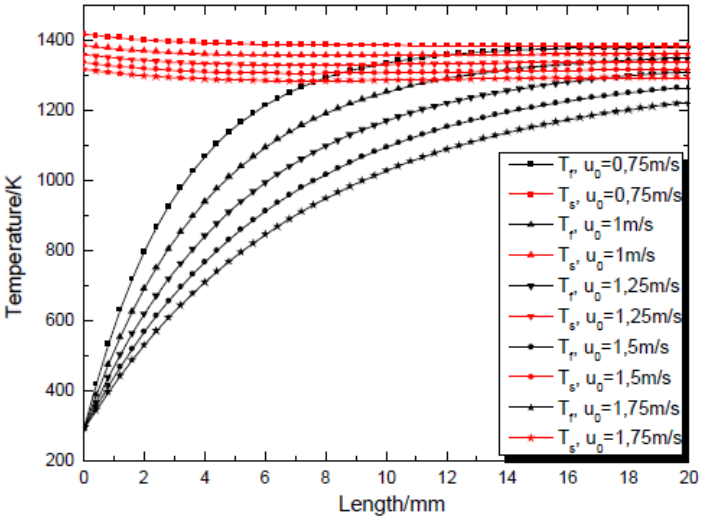


Fig. 13. The influence of air inlet velocity on the temperature distribution; $\varepsilon = 0.25$, $d_p = 0.025mm$, $qw = 1MW/m^2$, $\lambda_s = 118W/(m-K)$, $L = 20mm$.

Fig. 13 shows the effect of inlet air velocity on the temperature profiles. Five different air inlet velocities, 0.75, 1, 1.25, 1.5 and 1.75 m/s, were examined. The remaining parameters were kept unchanged from those used in Fig. 9. Qualitatively similar trends as discussed on the results shown in Fig. 9 were observed: the temperature of the solid matrix decreases slightly along the air flow direction but the air temperature increases rapidly. The bigger the air inlet velocity is, the lower the solid matrix temperature is. The solid matrix temperature of the heat absorbing surface is 1418,1 K when the air inlet velocity is set to 0.75 m/s, whereas the temperature is 1317,2 K when the air inlet velocity is se to 1.75 m/s.
Increasing the velocity impose decreasing the course the stage (the needed time to go through the solid matrix length from the inlet to the outlet), which make the accumulation of heat energy lower in the matrix, because the heat flux is constant $q_w = 1MW/m^2$. In the same position, the bigger the air inlet velocity is, the lower the air temperature is.
The steady-state assumption is imposed; all radiant energy input from the solar flux is carried away by the convective heat transfer as signified by the decreasing of temperature at the outlet.

**6. Conclusion**

One dimensional and steady incompressible air Flow through porous media has been investigated for a number of different parameters choosing B. Achenbach model, solves these equations by using the finite volume numerical method (FORTRAN code), and analyzes the typical influences of the heat inlet flux, thermal conductivity of solid matrix, porosity, air inlet thickness, and velocity on the temperature distributions yielding the following conclusions:

- The solid matrix temperature decreases or unchanged and the passing air temperature increases along the air downstream direction. The solid matrix temperature of the receiver heat absorbing surface is the highest in the whole receiver. The temperatures of the passing air are nonlinear along the air downstream direction.
- In the same position, the bigger the inlet heat flux is, the higher the solid matrix temperature is, the higher the air temperature is, the higher the temperature difference at the entrance between solid matrix and passing air temperature is.
- Quasi-Similar trends of the temperature distribution along the air flow direction for the solid matrix and the air when the thermal conductivity $\lambda$ increases. So, the diffusive flux has not a significant importance on the temperature distribution; because the most important heat flux is the convective flux.
- The solid matrix temperatures are unchanged with increasing porosity. In the same position, the bigger the porosity is, the lower the air temperature is, the higher the temperature difference between solid matrix and passing air is.
- In the same relative position, the bigger the thickness is, the lower the solid matrix temperature is, the higher the air temperature is, the lower the temperature difference between solid matrix and passing air is.
- At the outlet, the bigger the air inlet velocity is, the lower the solid matrix temperature and the air temperature is. In the same position, the bigger the air inlet velocity is, the lower the air temperature is.

## Reference


[1] Antonio L. Avila-Marin. Volumetric receivers in Solar Thermal Power Plants with Central Receiver System technology: A review. Solar Energy 85 (2011) 891 – 910. CIEMAT, Departamento de Energia, Avda. Complutense 22, E-28040 Madrid, Spain.

[2] R. Chacartegui et al. Alternative cycles based on carbon dioxide for central receiver solar power plants. Applied Thermal Engineering. 31 (2011) 872e879. Thermal Power Group (GMTS), Escuela Técnica Superior de Ingenieros, Camino de los descubrimientos s/n, 41092 Sevilla, Spain.

[3] Hennecke, K., Schwarzbozl et al. The Solar Power Tower Jülich: A Solar Thermal Power Plant For Test And Demonstration Of Air Receiver Technology. Proceedings of ISES Solar World Congress 2007: Solar Energy and Human Settlement.

[4] Renewable Energy Technology Characterizations. Office of Utility Technologies, Energy Efficiency and Renewable Energy. December 1997. Washington, D.C. 20585.

[5] Spiros Alexopoulos, Bernhard Hoffschmidt. Solar tower power plant in Germany and future perspectives of the development of the technology in Greece and Cyprus. Renewable Energy 35 (2010) 1352–1356. Solar-Institut Jülich (SIJ), FH Aachen, Aachen University of Applied Sciences, Heinrich-Mußmann-Str. 5, D-52428 Jülich, Germany.

[6] Amine Boudghene Stambouli. Promotion of renewable energies in Algeria: Strategies and perspectives. Renewable and Sustainable Energy Reviews 15 (2011) 1169–1181. University of Sciences and Technology of Oran, BP 1505, EL M'Naouer, Oran 31000, Algeria.

[7] Renewable Energy and Energy Efficiency Program. Produced by the ministry of energy and mines. Designed and printed by SATINFO, Sonelgaz Group Company. March 2011.

[8] Liu Deyou, Xu Chang, Wang Dingsheng, Bian Xingao, Guo Su. Study on the integrated control system at solar power tower plants. Proceedings of ISES Solar World Congress 2007: Solar Energy and Human Settlement.

[9] Manuel Romero et al. An Update on Solar Central Receiver Systems, Projects, and Technologies. Journal of Solar Energy Engineering. MAY 2002, MAY 2002, Vol. 124 / 99. Centro de Investigaciones Energéticas, Medioambientales y Tecnologicas, Avenida Complutense, 22, E 28040 Madrid, Spain.

[10] THOMAS FEND. High porosity materials as volumetric receivers for solar energetic. Optica Applicata, Vol. XL, No. 2, 2010.

[11] J. Karni, A. Kribus, R. Rubin, P. Doron. The “Porcupine”: A Novel High-Flux Absorber For Volumetric Solar Receivers. J. Solar Energy Engineering. Vol.120 / 85–95. The Weizmann Institute of Science Rehovot 76100, ISRAEL 1998.

[12] R. Pitz-Paal,+ B. Hoffschmidt, M. Bohmer And M. Becker. Experimental And Numerical Evaluation Of The Performance And Flow Stability Of Different Types Of Open Volumetric Absorbers Under Non-Homogeneous Irradiation. .Sular Energy Vol. 60, Nos. 3/4, pp. 135-150, Germany1997.

[13] Zhiyong Wu et al. Experimental and numerical studies of the pressure drop in ceramic foams for volumetric solar receiver applications. Applied Energy 87 (2010) 504–513. Institute of Electrical Engineering. Beijing, China.

[14] Chang Xu et al. Numerical investigation on porous media heat transfer in a solar tower receiver Renewable Energy 36 (2011) 1138e1144. College of Energy and Electricity, Hohai University, Nanjing, Jiangsu Province 210098, China.

[15] Suhas V.PantaKard. Numerical Heat Transfer and Fluid Flow. Himisphere Publishing Corporation. New York.